Published in final edited form as:
Circ Res. 2008 July 18; 103(2): 194–202. doi:10.1161/CIRCRESAHA.108.178590.

Engineering robust and functional vascular networks *in vivo* with human adult and cord blood-derived progenitor cells

Juan M. Melero-Martin[1], **Maria E. De Obaldia**[1], **Soo-Young Kang**[1], **Zia A. Khan**[1], **Lei Yuan**[2], **Peter Oettgen**[2], and **Joyce Bischoff**[1]

[1] Vascular Biology Program and Department of Surgery, Children's Hospital Boston, Harvard Medical School, Boston MA, USA

[2] Division of Cardiology, Beth Israel Deaconess Medical Center, Harvard Medical School, Boston MA, USA

Abstract

The success of therapeutic vascularization and tissue engineering will rely on our ability to create vascular networks using human cells that can be obtained readily, expanded safely *ex vivo* and produce robust vasculogenic activity *in vivo*. Here we describe the formation of functional microvascular beds in immunodeficient mice by co-implantation of human endothelial and mesenchymal progenitor cells (EPCs and MPCs) isolated from blood and bone marrow. Evaluation of implants after one week revealed an extensive network of human blood vessels containing erythrocytes, indicating the rapid formation of functional anastomoses within the host vasculature. The implanted EPCs were restricted to the luminal aspect of the vessels; MPCs were adjacent to lumens, confirming their role as perivascular cells. Importantly, the engineered vascular networks remained patent at 4 weeks *in vivo*. This rapid formation of long-lasting microvascular networks by postnatal progenitor cells obtained from non-invasive sources constitutes an important step forward in the development of clinical strategies for tissue vascularization.

Keywords

Vascular networks; endothelial progenitor cells; mesenchymal stem cells; mesenchymal progenitor cells; tissue engineering; regenerative medicine; vasculogenesis; angiogenesis

Introduction

Engineered tissues must have the capacity to generate a vascular network which rapidly form anastomoses with the host vasculature in order to guarantee adequate nutrients, gas exchange, and elimination of waste products [1]. Currently, there are no tissue-engineered (TE) constructs clinically available with an inherent microvascular bed, and therefore successes have been restricted to the replacement of relatively thin (skin) or avascular (cartilage) tissues, where post-implantation vascularization from the host is sufficient.

To overcome the problem of vascularization, strategies to promote ingrowth of microvessels by delivery of angiogenic molecules have been proposed [2-5]. However, rapid and complete

Corresponding Author: Dr. Joyce Bischoff, Vascular Biology Program and Department of Surgery, Children's Hospital Boston, Harvard Medical School, Boston, MA 02115, Tel.: (617) 919-2192, Fax: (617) 730-0231, joyce.bischoff@childrens.harvard.edu.

Disclosures: None.

vascularization of thick engineered tissues is likely to require an additional process of vasculogenesis [1, 6]. Towards this goal, the feasibility of engineering microvascular networks *in vivo* has been shown using human umbilical vein ECs (HUVECs) and human microvascular ECs (HDMECs) [7-9]; however, such autologous tissue-derived ECs present problems for wide clinical use, since they are difficult to obtain in sufficient quantities. These limitations have instigated the search for other sources of ECs, such as those derived from embryonic and adult stem and progenitor cells 6. For instance, endothelial cells derived from embryonic stem cells (ESCs) have been used to form blood vessels and to enhance the vascularization of engineered skeletal muscle constructs *in vivo* [10, 11]. However, the mechanisms controlling ESCs differentiation must be understood, and ethical issues surrounding their use must be resolved prior to their implementation in therapeutic strategies.

The identification of endothelial progenitor cells (EPCs) in blood presented an opportunity to non-invasively obtain ECs [12-14]. We and other authors have shown that adult and cord blood-derived EPCs have the required vasculogenic capacity to form functional vascular networks *in vivo* [15-17]. Importantly, these studies have also shown that in order to obtain stable and durable vascular networks, EPCs require co-implantation with perivascular cells. In our previous work, the role of perivascular cells was undertaken by smooth muscle cells (SMCs) isolated from human saphenous veins [15]. In the work by Au *et al*, the mouse embryonic cell line 10T1/2 served as the perivascular component of the vascular networks 16. However, neither source is suitable for clinical utilization: harvesting SMCs from healthy vasculature would impose serious morbidity in patients and murine-derived cell lines will not be used in humans. Therefore, to exploit the full vasculogenic potential of EPCs, we set out to establish clinically viable sources of perivascular cells. The ideal perivascular cells must present several key properties: 1) isolation with minimal donor site morbidity; 2) availability in sufficient quantities; and 3) immunological compatibility with the recipients [1]. Mesenchymal stem/progenitor cells (herein referred to as MPCs) [18] meet these requirements. MPCs can be isolated by minimally invasive procedures from a diversity of human tissues, including bone marrow 18, adult blood 19, umbilical cord blood [20-22], and adipose tissue [23]. Furthermore, MPCs undergo self-renewal, and therefore can potentially be expanded to sufficient quantities for tissue and organ regeneration [24].

Here we demonstrate that MPCs obtained from both human adult bone marrow and human cord blood can serve as perivascular cells for *in vivo* vasculogenesis. Subcutaneous co-implantation of EPCs and MPCs, suspended as single cells in Matrigel, into immunodeficient mice resulted in the creation of extensive microvascular beds that rapidly formed anastomoses with the host vasculature. This study constitutes a step forward in the clinical development of therapeutic vasculogenesis by showing the feasibility of using human adult and cord blood-derived progenitor cells as the basic cellular building blocks to create functional vascular networks *in vivo*.

Materials and methods

In vivo vasculogenesis assay

The formation of vascular networks *in vivo* was evaluated using a xenograft model as described [15]. A total of 1.9×10^6 cells was resuspended in 200 μl of ice-cold Phenol Red-free Matrigel™ (BD Bioscience, San Jose, CA), at ratios of 100:0, 80:20, 60:40, 40:60, 20:80 and 0:100 (EPCs:MPCs). The mixture was implanted on the back of a six-week-old male athymic nu/nu mouse (Massachusetts General Hospital, Boston, MA) by subcutaneous injection using a 25-gauge needle. Implants of Matrigel alone served as controls. One implant was injected per mouse. Each experimental condition was performed with 4 mice.

An expanded Materials and Methods section, available at http://circres.ahajournals.org, describes cell isolation and expansion, flow cytometry, western blot analysis, differentiation assays, histology and immunohistochemistry, retroviral transduction, luciferase assay, microvessel density evaluation, and statistical analysis.

Results

Isolation of EPCs and MPCs

Cord blood-derived EPCs (cbEPCs) (Fig. 1a) and adult blood EPCs (abEPCs) were isolated from the MNC fraction of human blood samples and purified by CD31-selection as described (see Supplementary Figs. 1 and 12 online for morphology of cbEPCs and abEPCs respectively) [15]. MPCs were isolated from the MNC fractions of human bone marrow samples (bmMPCs) and human cord blood samples (cbMPCs). bmMPCs adhered rapidly to the culture plates and proliferated until confluent while cbMPCs emerged more slowly, forming mesenchymal-like colonies after one week (Supplementary Fig. 1 online). cbMPC colonies were selected with cloning rings and expanded. Both bmMPCs (Fig. 1b) and cbMPCs (Fig. 1c) presented spindle morphology characteristic of mesenchymal cells in culture [18].

cbEPCs and MPCs were grown in EPC-medium and MPC-medium respectively and their expansion potentials estimated by the cumulative cell numbers obtained from 25 mL of either cord blood or bone marrow samples after 25, 40 and 60 days in culture (Fig. 1d). Remarkably, up to 10^{13} cbEPCs and 10^{11} bmMPCs were obtained after 40 days, consistent with previous studies [13, 15]. The number of cells continued to increase so that at 60 days there were an estimated 10^{18} cbEPCs and 10^{14} bmMPCs respectively. In the case of cbMPCs, a longer culture period was necessary to obtain such numbers. The apparent decreased number of cbMPCs was likely due to the smaller number of MPCs in cord blood samples (typically 1-2 colonies/25 mL; data not shown) as compared to bone marrow samples, where the majority of the adherent cells contributed to the final bmMPC population (Supplementary Fig. 1 online).

The phenotype of the MPCs was confirmed by three methods. Flow cytometry (Fig. 1e) showed that bmMPCs and cbMPCs uniformly expressed the mesenchymal marker CD90 and were negative for the endothelial marker CD31 and the hematopoietic marker CD45 (see further flow cytometric evaluations in Supplementary Fig. 2 online). cbEPCs served as a control. Western blot analyses (Fig. 1f, g) confirmed the mesenchymal phenotype of bmMPCs and cbMPCs (expression of α-SMA and calponin) and the endothelial phenotype of cbEPCs (expression of CD31 and VE-cadherin). These data were extended by indirect immunofluorescent staining (Supplementary Fig. 3 online): bmMPCs and cbMPCs were shown to express the mesenchymal markers α-SMA, calponin, and NG_2 but not the EC markers CD31, VE-cadherin and vWF. Importantly, smooth muscle myosin heavy chain (smMHC), a specific marker of differentiated smooth muscle cells [25, 26], was found in mature SMCs but not in any of the MPCs.

The ability of MPCs to differentiate into multiple mesenchymal lineages was evaluated *in vitro* using well-established protocols [18]. Both bmMPCs and cbMPCs differentiated into osteocytes and chondrocytes as shown by the expression of alkaline phosphatase (osteogenesis; Fig. 2a, b) and glycosaminoglycan deposition in pellet cultures (chondrogenesis; Fig. 2c, d) respectively (see also Supplementary Fig. 4). Adipogenesis was only evident with bmMPCs (Fig. 2e), and not in cbMPCs (Fig. 2f). This loss of adipogenic potential, reported for other mesenchymal cells in culture [27, 28], was attributed to the extensive expansion that these cells required due to their lower presence in cord blood samples (the earliest cbMPCs were tested for adipogenesis was at passage 5).

Since we intended to test MPCs as perivascular cells to engineer microvessel networks, we evaluated the ability of MPCs to differentiate towards a smooth muscle phenotype. As already shown, MPCs and mature SMCs shared a number of cellular markers including α-SMA, calponin, NG_2, and PDGF-Rβ (Supplementary Fig. 5 online). Although the definitive smooth muscle cell marker smMHC was absent in MPCs (Fig. 2g, h), both bmMPCs and cbMPCs were induced to express smMHC when directly co-cultured with cbEPCs (Fig. 2i, j). Importantly, induction did not occur when MPCs were indirectly co-cultured with cbEPCs using a Transwell culture system (Supplementary Fig. 6 online), consistent with previous reports that showed direct contact with endothelial cells is required for mesenchymal cell differentiation into SMCs [29, 30].

In vivo formation of human vascular networks

We have previously demonstrated the vasculogenic capacity of blood-derived EPCs both *in vitro* and *in vivo* [15, 31]. In these studies, the presence of vascular smooth muscle cells was required for formation of vascular networks. To answer the question of whether MPCs could be used instead of SMCs, we implanted different combinations of cbEPCs and MPCs (either bmMPCs or cbMPCs) into nude mice for one week (Fig. 3). A total of 1.9×10^6 cells was resuspended in 200 μl of Matrigel, using ratios of 100:0, 80:20, 60:40, 40:60, 20:80 and 0:100 (% cbEPCs:% MPCs), and injected subcutaneously. After harvesting the Matrigel implants (Fig. 3a-c), Hematoxylin and eosin (H&E) staining revealed numerous vessels containing erythrocytes in implants containing both cbEPCs and MPCs (Fig. 3e, g). The structures stained positive for human CD31 (Fig. 3d, f), confirming the lumens were lined by the implanted cells (the specificity of the anti-human CD31 antibody is shown in Supplementary Fig. 9 online). Implants of Matrigel alone were devoid of vessels (Supplementary Fig. 7 online) indicating the Matrigel itself was not responsible for the presence of vascular structures. As expected [15], implants with cbEPCs alone (Fig.3h) failed to form microvessels. Implants with only MPCs (Fig. 3i, j) presented infiltration of murine blood capillaries, but no human microvessels (Supplementary Fig. 9 online). The ability of human MPCs to recruit murine vessels into Matrigel may be explained by the secretion of VEGF from MPCs but not cbEPCs (Supplementary Fig. 8 online).

Microvessel density was determined by quantification of lumens containing red blood cells (Fig.3k). The extent of the engineered vascular networks was influenced by the ratio of EPCs to MPCs (Fig. 3k). A progressive increase in MPCs resulted in increased microvessel density and more consistent vascularization (Supplementary Table 1 online). When the ratio of EPC:MPC was 40:60, an average density of 119 ± 33 vessels/mm^2 and 117 ± 32 vessels/mm^2 with bmMPCs or cbMPCs, respectively, was achieved in all implants. These densities were significantly higher ($P< 0.05$) than those observed with MPCs alone, reaffirming the necessity of the endothelial component for the formation of human vessels in the implants.

Assembly of endothelial and mesenchymal progenitor cells in the vascular bed

In addition to the human CD31-positive lumenal structures, the engineered vessels were characterized by α-SMA staining of perivascular cells (Fig. 4a, b). With bmMPCs or cbMPCs, α-SMA-positive cells were detected both in proximity and adjacent to lumenal structures, suggesting an ongoing process of perivascular cell recruitment during vessel maturation [32-34]. In order to determine more precisely the contribution of each cell type, we implanted GFP-labeled cbEPCs with unlabeled MPCs. Anti-GFP staining showed cbEPCs restricted to lumenal positions in the microvessel networks, while anti-α-SMA staining showed that the GFP-labeled vessels were covered by perivascular cells; this observation was valid with both sources of MPCs (Fig. 4c, d). Projections of whole-mount staining showed that the GFP-expressing cells formed extensive networks throughout the implants (Fig. 4e). Conversely, we implanted GFP-labeled bmMPCs with unlabeled cbEPCs to

identify input MPCs without relying on anti-α-SMA. Sections were stained with anti-GFP and anti-CD31 antibodies: GFP-expressing cells were detected as perivascular cells surrounding human CD31+ lumens and as individual cells dispersed throughout the Matrigel implants (Fig. 4f).

Durability of the vascular bed

To test the durability of the engineered vascular beds *in vivo*, we evaluated implants of cbEPCs-bmMPCs (40:60) at 7, 14, 21 and 28 days after xenografting (Fig. 5). H&E staining revealed the presence of lumenal structures containing erythrocytes in all implants at each time point (Fig. 5a-d). Microvessel quantification (Fig. 5e) revealed an initial reduction (statistically non-significant; P=0.105) in the number of patent blood vessels from 119 ± 33 vessels/mm^2 at day 7 to 83 ± 16 vessels/mm^2 at day 14. Microvessel densities remained stable thereafter (87 ± 21 vessels/mm^2 and 87 ± 32 vessels/mm^2 at days 21 and 28 respectively).

To further evaluate the engineered vascular bed, we used a luciferase-based imaging system to monitor perfusion of the Matrigel implants. cbEPCs were infected with lentivirus-associated vector encoding luciferase and implanted into immunodeficient mice in the presence or absence of bmMPCs. At one week and four weeks, mice were given the substrate, luciferin, by intraperitoneal injection (Fig. 5f). No bioluminescence was detected in implants with luciferase-expressing cbEPC alone, indicating that the substrate did not diffuse into the Matrigel. In contrast, a strong bioluminescent signal was detected in xenografts in which bmMPCs were co-implanted. This result, coupled with parallel histological data, confirmed that the presence of MPCs was crucial to achieve rapid perfusion of the implants. Importantly, the luciferase-dependent signal was still detected 4 weeks after implantation, a further indication of the long-lasting nature of the engineered vessels.

The cells within the Matrigel implants appeared to undergo a process of *in vivo* remodeling characterized by stabilization of total cellularity (Supplementary Fig. 10 online) and progressive restriction of α-SMA-expressing cells to perivascular locations (Fig. 5g-j), as expected in normal stabilized vasculature [34]. Finally, after 28 days *in vivo*, adipocytes were identified by staining with an anti-perilipin antibody (Supplementary Fig. 11 online), suggesting a process of integration between the implants and the surrounding murine adipose tissue [35].

Vascular network formation using adult progenitor cells

We previously showed that adult peripheral blood-derived EPCs (abEPCs) combined with mature SMCs at a ratio of 4:1 (EPCs:SMCs), are vasculogenic *in vivo*, yet required higher seeding densities to achieve microvessel densities similar to that obtained with cbEPCs [15]. This apparently lower vasculogenic capacity of abEPCs has been suggested recently by others [16]. We hypothesized that the combination of adult bmMPCs and abEPCs at an *optimized ratio* (Fig. 3k) would yield a high density vascular network. Indeed, there are no previous reports on adult human bmMPCs and abEPCs in the context of *in vivo* vasculogenesis. To evaluate this interaction, we isolated abEPCs as described 13-15, and confirmed their endothelial phenotype (Supplementary Fig. 12 online).

We implanted a total of 1.9×10^6 cells (40% abEPCs and 60% bmMPCs) in Matrigel by subcutaneous injection into immunodeficient mice (Fig. 6). After harvesting the implants at 7 days (n=4), H&E staining consistently showed an extensive presence of blood vessels containing erythrocytes (Fig. 6a, b). In addition, the lumenal structures stained positive for human CD31 (Fig. 6d), confirming the lumens were formed by the implanted human

abEPCs. Quantification of microvessel density (Fig. 6c) revealed that the use of 40% abEPCs resulted in a statistically significant ($P<0.05$) increase in the number of blood vessels (86 ± 26 vessels/mm^2) as compared to implants with bmMPCs alone (34 ± 25 vessels/mm^2). Moreover, the difference between implants composed of abEPCs:bmMPCs and those of cbEPCs:bmMPCs (119 ± 33 vessels/mm^2) was not statistically significant ($P=0.158$), indicating that the presence of bmMPCs supported the vasculogenic properties of abEPCs to the same extent as was achieved with cbEPCs. These results show that a two cell system composed of human adult EPCs and MPCs exhibit the same robust in vivo vasculogenic activity as cbEPCs combined with adult bmMPCs, which is in contrast to conclusions drawn from experiments reported by others using a murine 10T1/2 cell line[16].

Discussion

Here, we show that human postnatal EPCs and MPCs isolated from either blood or bone marrow have an inherent vasculogenic ability that can be exploited to create functional microvascular networks *in vivo*. Using Matrigel as a supporting scaffold [15], we have shown that co-implantation of EPCs with either bmMPCs or cbMPCs into immunodeficient mice resulted in formation of extensive vascular networks after one week. The presence of human EPC-lined lumens containing erythrocytes (>100 vessels/mm^2) throughout the implants indicated not only a process of vasculogenesis from the two cell types, but also the formation of functional anastomoses with the host circulatory system. In addition, MPCs were shown to reside in perivascular locations around the engineered lumens, confirming their active participation in blood vessel assembly. In vitro, MPCs were shown to differentiate into smMHC-positive cells when co-cultured with EPCs, an indication that the MPCs achieved a mature smooth muscle phenotype. In a recent report, human mesenchymal stem cells combined with HUVECs were shown to facilitate blood vessel assembly and adopt a perivascular location [36], but our study differs from this report in that we show EPCs from either adult or cord blood, combined with MPCs from adult bone marrow or cord blood, form robust vascular networks in vivo. The extent of the engineered vascular networks was highly influenced by the ratio of EPCs to MPCs, with a progressive increase in vessel density and consistency of vascularized implants achieved when the contribution of MPCs was raised to 60% (Fig. 3). This was true for both abEPCs and cbEPCs (Fig. 6), demonstrating that both cord blood and adult peripheral blood are excellent sources of endothelial cells for tissue vascularization.

Previous studies suggested the possibility of using mature ECs derived from vascular tissue to create microvascular networks [7-9, 37]. However, the clinical use of mature ECs derived from autologous vascular tissue is limited by the difficulty of obtaining sufficient quantities of cells with minimal donor site morbidity [1]. Human ESCs have unlimited expansion capacity, but the therapeutic use of ESCs-derived ECs remains years away from the clinic. Most of these hurdles would be resolved if postnatal progenitor cells with expansion and functional potential were available from individual patients or from dedicated cell banks. In this regard, the *in vitro* expansion of blood-derived EPCs [12-15] and the recent confirmation of their ability to form vascular networks *in vivo* [15-17] have constituted major steps forward to resolve the problem of EC sourcing for therapeutic vasculogenesis.

Importantly, these studies have also shown that in order to produce high density and stable vascular networks, EPCs require co-implantation with perivascular cells. This is consistent with the literature showing interactions between ECs and perivascular cells in the blood vessel wall are critical for normal vascular development [32-34]. In previous attempts to create vascular networks with blood-derived EPCs, either mature SMCs [15] or the mouse embryonic cell line 10T1/2 [16] were used to serve as perivascular cells; however, neither source is suitable for clinical application. Therefore, identification of MPCs as a readily obtainable

perivascular cell source to partner *in vivo* with EPCs constitutes a crucial step in the development of therapeutic vasculogenesis. The numbers of human MPCs we were able to obtain in this study are likely to exceed, in the case of bone marrow, and be sufficient, in the case of cord blood, what would be needed for most autologous regenerative therapies.

This study has shown that successful *in vivo* vascularization depends on several distinct cellular functions. Firstly, both EPCs and MPCs must be present to initiate vasculogenesis, a process that was characterized by the formation of lumenal structures composed of human EPCs surrounded by α-SMA positive mesenchymal cells. Secondly, an angiogenic response from the host vasculature is needed so that host vessels will be available to form anastomoses with the nascent vasculature. In this regard, we propose that the implanted MPCs stimulated the host angiogenic response. This is based on 1) the ability of bmMPCs alone to recruit murine vessels into the Matrigel implant and 2) the secretion of VEGF from MPCs *in vitro* (Supplementary Fig. 8 online). EPCs did not secrete VEGF and did not stimulate murine vessel infiltration. Vascularization is achieved when the angiogenic and vasculogenic blood vessels meet, form anastomoses, and establish perfusion of the implants. The fact that perfusion occurred was supported by the presence of erythrocytes within the newly formed vasculature and the delivery of luciferin substrate from the peritoneal cavity to Matrigel implants containing both cbEPCs and bmMPCs. Subsequently, a process reminiscent of *in vivo* remodeling, characterized by a progressive restriction of α-SMA-expressing cells to perivascular locations, was seen, suggesting a stabilized vasculature [34]. Whether factors secreted or presented by MPCs contribute to such stabilization would be important to elucidate in a future study. Finally, our engineered vascular networks were patent for up to 4 weeks *in vivo*, confirming the capacity of EPC/MPC-derived vasculature to remain stable and functional [16].

In summary, we have demonstrated the feasibility of engineering vascular networks *in vivo* with human postnatal progenitor cells that can be obtained by noninvasive procedures. In addition, we suggest that this murine model of human vasculogenesis is ideally suited for future studies on the cellular and molecular components of microvessel development, pathologic neovascular responses, and for the development of strategies to enhance neovascularization of engineered human tissues and organs. Further efforts are required to implement these vascularization strategies into tissue regeneration and tissue engineering applications.

Acknowledgments

We thank Dr. Joseph C. Wu for providing construct of pUb-fluc-GFP (Department of Radiology and Molecular Imaging Program, Stanford University School of Medicine), Dr. Masanori Aikawa for providing SMCs (Brigham and Women's Hospital), Elke Pravda for confocal microscopy, Sandra R. Smith for VEGF analysis, Jill Wylie-Sears for technical assistance, and Kristin Johnson for figure preparation.

Sources of funding: US Army Medical Research and Materiel Command (W81XWH-05-1-0115).

References

1. Jain RK, Au P, Tam J, Duda DG, Fukumura D. Engineering vascularized tissue. Nat Biotechnol 2005;23:821–823. [PubMed: 16003365]
2. Isner JM, Asahara T. Angiogenesis and vasculogenesis as therapeutic strategies for postnatal neovascularization. J Clin Invest 1999;103:1231–1236. [PubMed: 10225965]
3. Isner JM, Pieczek A, Schainfeld R, Blair R, Haley L, Asahara T, Rosenfield K, Razvi S, Walsh K, Symes JF. Clinical evidence of angiogenesis after arterial gene transfer of phVEGF165 in patient with ischaemic limb. Lancet 1996;348:370–374. [PubMed: 8709735]

4. Lee H, Cusick RA, Browne F, Ho Kim T, Ma PX, Utsunomiya H, Langer R, Vacanti JP. Local delivery of basic fibroblast growth factor increases both angiogenesis and engraftment of hepatocytes in tissue-engineered polymer devices. Transplantation 2002;73:1589–1593. [PubMed: 12042644]
5. Li X, Tjwa M, Moons L, Fons P, Noel A, Ny A, Zhou JM, Lennartsson J, Li H, Luttun A, Ponten A, Devy L, Bouche A, Oh H, Manderveld A, Blacher S, Communi D, Savi P, Bono F, Dewerchin M, Foidart JM, Autiero M, Herbert JM, Collen D, Heldin CH, Eriksson U, Carmeliet P. Revascularization of ischemic tissues by PDGF-CC via effects on endothelial cells and their progenitors. J Clin Invest 2005;115:118–127. [PubMed: 15630451]
6. Rafii S, Lyden D. Therapeutic stem and progenitor cell transplantation for organ vascularization and regeneration. Nat Med 2003;9:702–712. [PubMed: 12778169]
7. Koike N, Fukumura D, Gralla O, Au P, Schechner JS, Jain RK. Tissue engineering: creation of long-lasting blood vessels. Nature 2004;428:138–139. [PubMed: 15014486]
8. Nor JE, Peters MC, Christensen JB, Sutorik MM, Linn S, Khan MK, Addison CL, Mooney DJ, Polverini PJ. Engineering and characterization of functional human microvessels in immunodeficient mice. Lab Invest 2001;81:453–463. [PubMed: 11304564]
9. Schechner JS, Nath AK, Zheng L, Kluger MS, Hughes CC, Sierra-Honigmann MR, Lorber MI, Tellides G, Kashgarian M, Bothwell AL, Pober JS. In vivo formation of complex microvessels lined by human endothelial cells in an immunodeficient mouse. Proc Natl Acad Sci U S A 2000;97:9191–9196. [PubMed: 10890921]
10. Levenberg S, Rouwkema J, Macdonald M, Garfein ES, Kohane DS, Darland DC, Marini R, van Blitterswijk CA, Mulligan RC, D'Amore PA, Langer R. Engineering vascularized skeletal muscle tissue. Nat Biotechnol 2005;23:879–884. [PubMed: 15965465]
11. Wang ZZ, Au P, Chen T, Shao Y, Daheron LM, Bai H, Arzigian M, Fukumura D, Jain RK, Scadden DT. Endothelial cells derived from human embryonic stem cells form durable blood vessels in vivo. Nat Biotechnol 2007;25:317–318. [PubMed: 17322871]
12. Asahara T, Murohara T, Sullivan A, Silver M, van der Zee R, Li T, Witzenbichler B, Schatteman G, Isner JM. Isolation of putative progenitor endothelial cells for angiogenesis. Science 1997;275:964–967. [PubMed: 9020076]
13. Ingram DA, Mead LE, Tanaka H, Meade V, Fenoglio A, Mortell K, Pollok K, Ferkowicz MJ, Gilley D, Yoder MC. Identification of a novel hierarchy of endothelial progenitor cells using human peripheral and umbilical cord blood. Blood 2004;104:2752–2760. [PubMed: 15226175]
14. Lin Y, Weisdorf DJ, Solovey A, Hebbel RP. Origins of circulating endothelial cells and endothelial outgrowth from blood. J Clin Invest 2000;105:71–77. [PubMed: 10619863]
15. Melero-Martin JM, Khan ZA, Picard A, Wu X, Paruchuri S, Bischoff J. In vivo vasculogenic potential of human blood-derived endothelial progenitor cells. Blood 2007;109:4761–4768. [PubMed: 17327403]
16. Au P, Daheron LM, Duda DG, Cohen KS, Tyrrell JA, Lanning RM, Fukumura D, Scadden DT, Jain RK. Differential in vivo potential of endothelial progenitor cells from human umbilical cord blood and adult peripheral blood to form functional long-lasting vessels. Blood 2008;111:1302–5. [PubMed: 17993613]
17. Yoder MC, Mead LE, Prater D, Krier TR, Mroueh KN, Li F, Krasich R, Temm CJ, Prchal JT, Ingram DA. Redefining endothelial progenitor cells via clonal analysis and hematopoietic stem/progenitor cell principals. Blood 2007;109:1801–1809. [PubMed: 17053059]
18. Pittenger MF, Mackay AM, Beck SC, Jaiswal RK, Douglas R, Mosca JD, Moorman MA, Simonetti DW, Craig S, Marshak DR. Multilineage potential of adult human mesenchymal stem cells. Science 1999;284:143–147. [PubMed: 10102814]
19. Simper D, Stalboerger PG, Panetta CJ, Wang S, Caplice NM. Smooth muscle progenitor cells in human blood. Circulation 2002;106:1199–1204. [PubMed: 12208793]
20. Kim JW, Kim SY, Park SY, Kim YM, Kim JM, Lee MH, Ryu HM. Mesenchymal progenitor cells in the human umbilical cord. Ann Hematol 2004;83:733–738. [PubMed: 15372203]
21. Le Ricousse-Roussanne S, Barateau V, Contreres JO, Boval B, Kraus-Berthier L, Tobelem G. Ex vivo differentiated endothelial and smooth muscle cells from human cord blood progenitors home to the angiogenic tumor vasculature. Cardiovasc Res 2004;62:176–184. [PubMed: 15023564]

22. Lee OK, Kuo TK, Chen WM, Lee KD, Hsieh SL, Chen TH. Isolation of multipotent mesenchymal stem cells from umbilical cord blood. Blood 2004;103:1669–1675. [PubMed: 14576065]
23. Traktuev D, Merfeld-Clauss S, Li J, Kolonin M, Arap W, Pasqualini R, Johnstone BH, March KL. A Population of Multipotent CD34-Positive Adipose Stromal Cells Share Pericyte and Mesenchymal Surface Markers, Reside in a Periendothelial Location, and Stabilize Endothelial Networks. Circ Res 2008;102:77–85. [PubMed: 17967785]
24. Marion NW, Mao JJ. Mesenchymal stem cells and tissue engineering. Methods Enzymol 2006;420:339–361. [PubMed: 17161705]
25. Madsen CS, Regan CP, Hungerford JE, White SL, Manabe I, Owens GK. Smooth muscle-specific expression of the smooth muscle myosin heavy chain gene in transgenic mice requires 5′-flanking and first intronic DNA sequence. Circ Res 1998;82:908–917. [PubMed: 9576110]
26. Miano JM, Cserjesi P, Ligon KL, Periasamy M, Olson EN. Smooth muscle myosin heavy chain exclusively marks the smooth muscle lineage during mouse embryogenesis. Circ Res 1994;75:803–812. [PubMed: 7923625]
27. Digirolamo CM, Stokes D, Colter D, Phinney DG, Class R, Prockop DJ. Propagation and senescence of human marrow stromal cells in culture: a simple colony-forming assay identifies samples with the greatest potential to propagate and differentiate. Br J Haematol 1999;107:275–281. [PubMed: 10583212]
28. Wall ME, Bernacki SH, Loboa EG. Effects of serial passaging on the adipogenic and osteogenic differentiation potential of adipose-derived human mesenchymal stem cells. Tissue Eng 2007;13:1291–1298. [PubMed: 17518709]
29. Antonelli-Orlidge A, Saunders KB, Smith SR, D'Amore PA. An activated form of transforming growth factor beta is produced by cocultures of endothelial cells and pericytes. Proc Natl Acad Sci U S A 1989;86:4544–4548. [PubMed: 2734305]
30. Hirschi KK, Rohovsky SA, D'Amore PA. PDGF, TGF-beta, and heterotypic cell-cell interactions mediate endothelial cell-induced recruitment of 10T1/2 cells and their differentiation to a smooth muscle fate. J Cell Biol 1998;141:805–814. [PubMed: 9566978]
31. Wu X, Rabkin-Aikawa E, Guleserian KJ, Perry TE, Masuda Y, Sutherland FW, Schoen FJ, Mayer JE Jr, Bischoff J. Tissue-engineered microvessels on three-dimensional biodegradable scaffolds using human endothelial progenitor cells. Am J Physiol Heart Circ Physiol 2004;287:H480–487. [PubMed: 15277191]
32. Darland DC, D'Amore PA. Blood vessel maturation: vascular development comes of age. J Clin Invest 1999;103:157–158. [PubMed: 9916126]
33. Folkman J, D'Amore PA. Blood vessel formation: what is its molecular basis? Cell 1996;87:1153–1155. [PubMed: 8980221]
34. Jain RK. Molecular regulation of vessel maturation. Nat Med 2003;9:685–693. [PubMed: 12778167]
35. Fukumura D, Ushiyama A, Duda DG, Xu L, Tam J, Krishna V, Chatterjee K, Garkavtsev I, Jain RK. Paracrine regulation of angiogenesis and adipocyte differentiation during in vivo adipogenesis. Circ Res 2003;93:e88–97. [PubMed: 14525808]
36. Au P, Tam J, Fukumura D, Jain RK. Bone marrow derived mesenchymal stem cells facilitate engineering of long-lasting functional vasculature. Blood 2008;111:4551–8. [PubMed: 18256324]
37. Shepherd BR, Chen HY, Smith CM, Gruionu G, Williams SK, Hoying JB. Rapid perfusion and network remodeling in a microvascular construct after implantation. Arterioscler Thromb Vasc Biol 2004;24:898–904. [PubMed: 14988090]

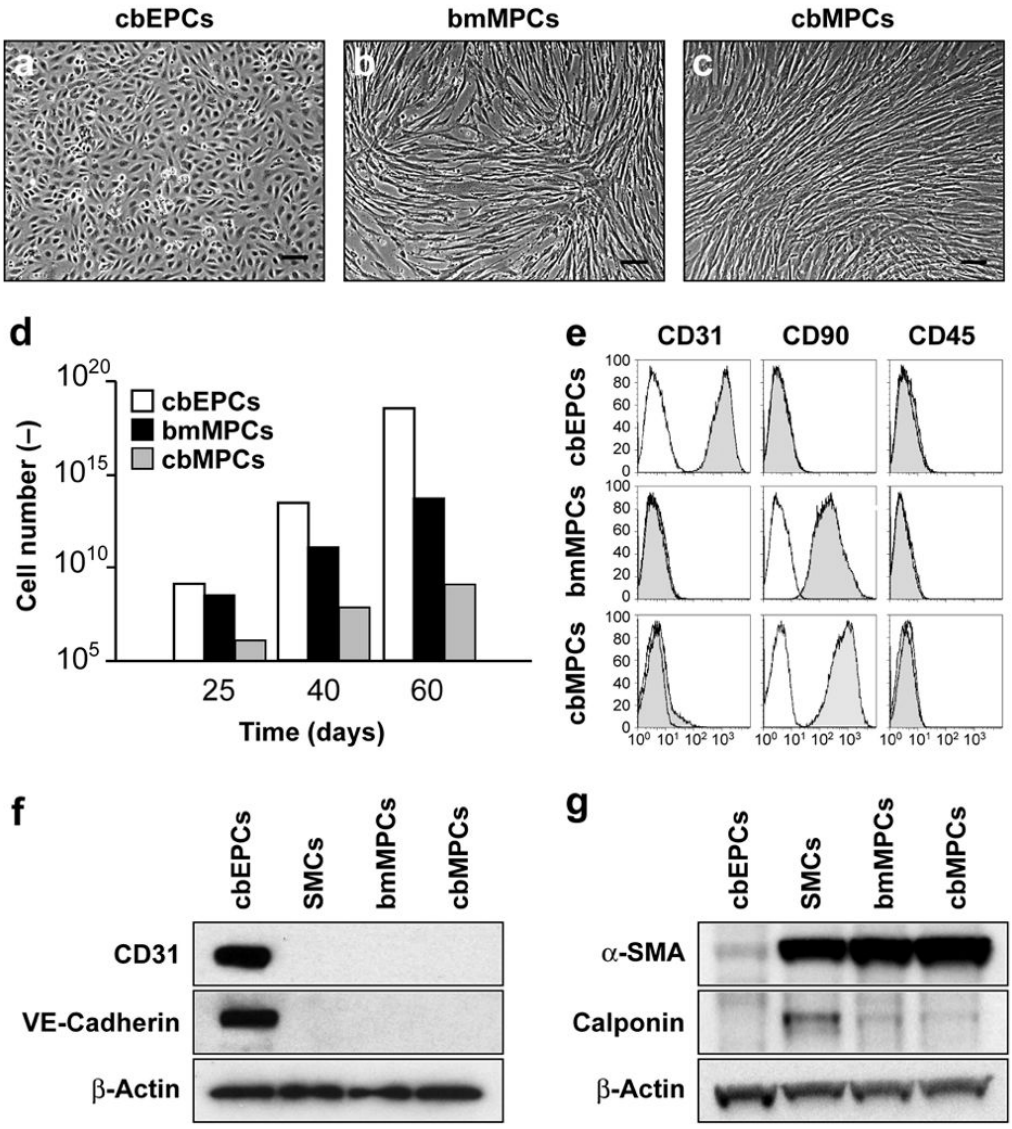

Figure 1. Phenotypic characterization

of EPCs and MPCs. (a) cbEPCs presented typical cobblestone morphology, while both (b) bMPCs and (c) cbMPCs presented spindle morphology characteristic of mesenchymal cells in culture (scale bars, 100 μm). (d) cbEPCs and MPCs were serially passaged and their *in vitro* expansion potential estimated by the accumulative cell numbers obtained from 25 mL of either cord blood or bone marrow samples. (e) Flow cytometric analysis of cbEPCs, bmMPCs and cbMPCs for the endothelial marker CD31, mesenchymal marker CD90, and hematopoietic marker CD45. Solid gray histograms represent cells stained with fluorescent antibodies. Isotype-matched controls are overlaid in a black line on each histogram. Western blot analyses of cbEPCs, bmMPCs and cbMPCs for (f) endothelial markers CD31, and VE-cadherin, and (g) mesenchymal markers α-SMA, and Calponin. Expression of β-actin shows equal protein loading. SMCs isolated from human saphenous vein served as control.

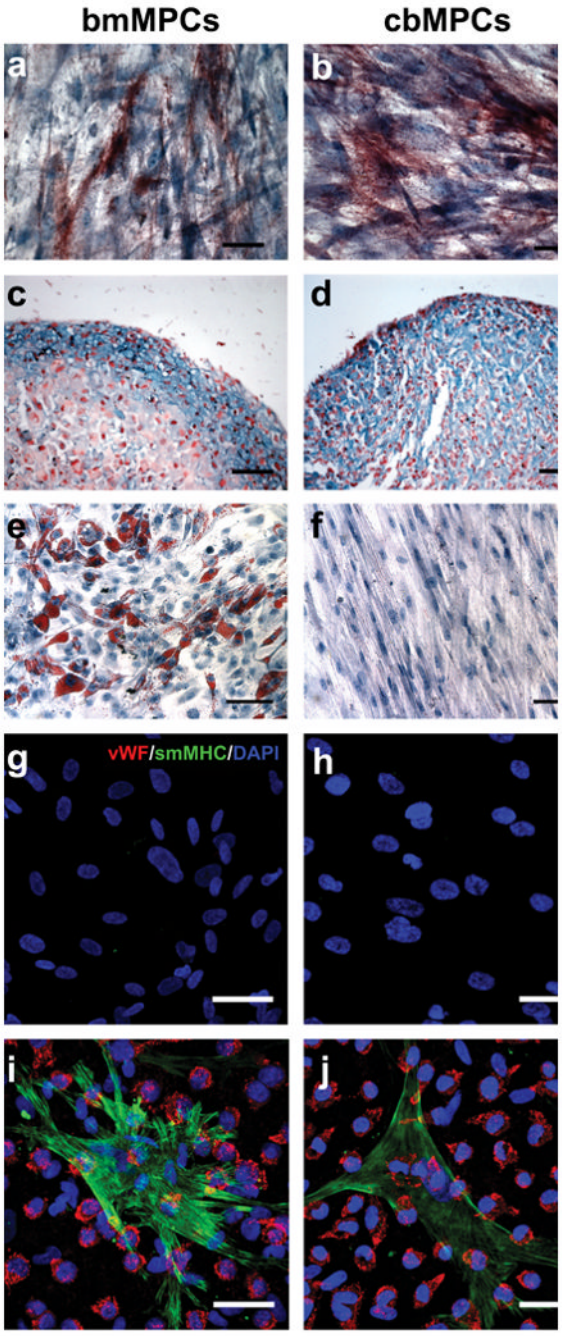

Figure 2. Multilineage differentiation of MPCs

(a) bmMPCs and (b) cbMPCs differentiation into osteocytes was revealed by alkaline phosphatase staining. (c) bmMPCs and (d) cbMPCs differentiation into chondrocytes was revealed by the presence of glycosaminoglycans, detected by Alcian Blue staining. The presence of adipocytes was assessed by Oil Red O staining, and it was evident in (e) bmMPCs, but absent in (f) cbMPCs. Smooth muscle cell differentiation was evaluated by culturing MPCs in the absence or presence of cbEPCs (1:1 EPCs to MPCs ratio) for 7 days in EPC-medium. Induction of SMC phenotype was assessed by the expression of smMHC. Immunofluorescence staining with anti-vWF-Texas-Red and anti-smMHC-FITC, as well as nuclear staining with DAPI, revealed that smMHC was absent in both (g) bmMPCs and (h)

cbMPCs, but it was induced in MPCs when co-cultured with cbEPCs (i, j). Scale bars correspond to 200 μm (e and f) and 50 μm (a-d and g-j).

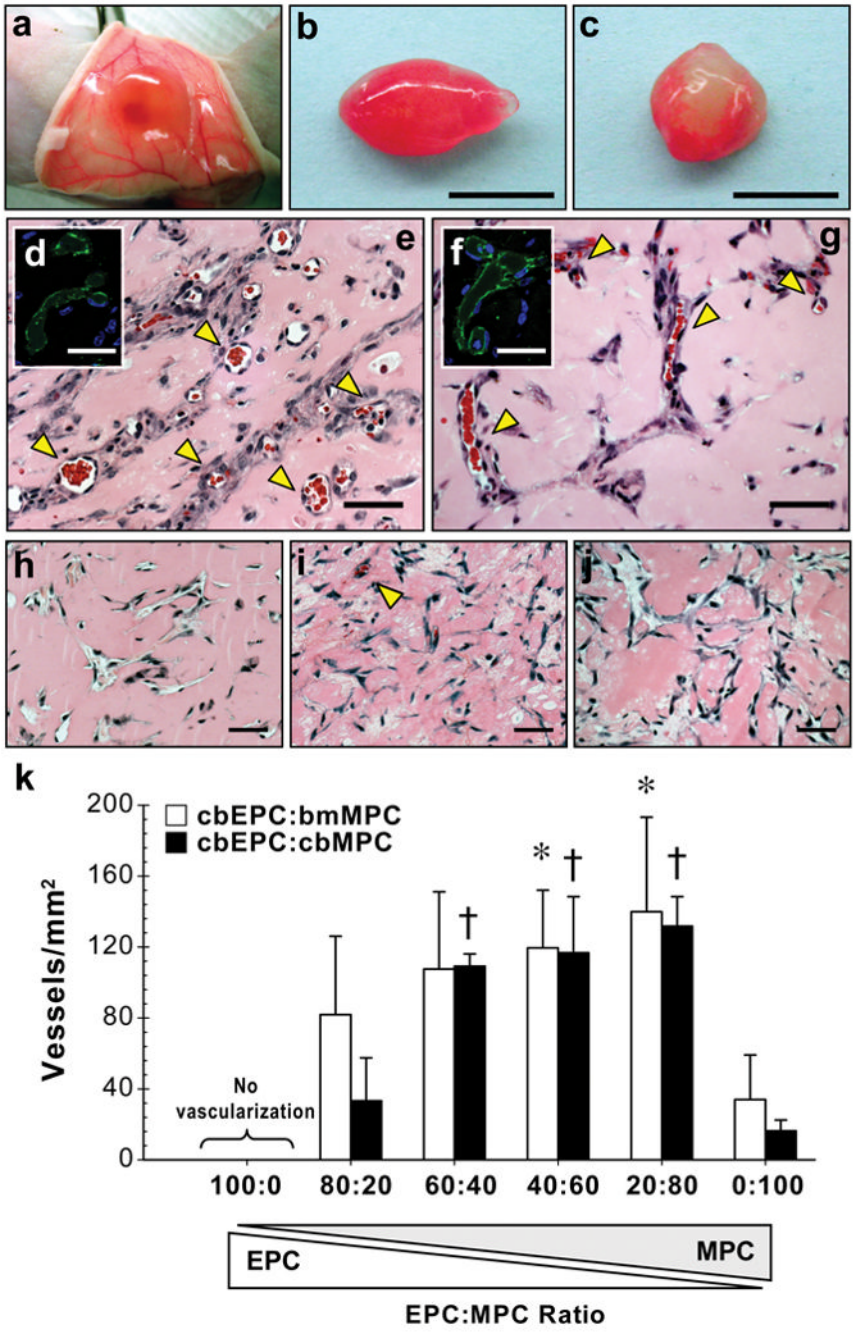

Figure 3. Formation of vascular networks *in vivo* with EPCs and MPCs

A total of 1.9×10^6 cells was resuspended in 200 μl of Matrigel using different ratios of cbEPCs and MPCs, and implanted on the back of six-week-old nu/nu mice by subcutaneous injection. Implants were harvested after 7 days and stained with H&E. (a, b) Macroscopic view of explanted Matrigel plugs seeded with 40% cbEPCs:60% bmMPCs and (c) 40% cbEPCs:60% cbMPCs (scale bars, 5 mm). (e, g) H&E staining revealed the presence of lumenal structures containing erythrocytes (yellow arrow heads) in implants where both cells types (cbEPCs and MPCs; 40:60) were used, but not in implants where (h) cbEPCs, (i) bmMPCs, and (j) cbMPCs were used alone (scale bars, 50 μm). Microvessels stained positive for human CD31 (d, f) (scale bars, 30 μm). Images are representative of implants

harvested from at least four different mice. (k) Quantification of microvessel density was performed by counting erythrocyte-filled vessels in implants with ratios of 100:0, 80:20, 60:40, 40:60, 20:80 and 0:100 (cbEPCs:MPCs; n≥4 each condition). Each bar represents the mean ± S.D. (vessels/mm^2) obtained from vascularized implants. * $P < .05$ compared to implants with bmMPCs alone (n=4). † $P < .05$ compared to implants with cbMPCs alone (n=4).

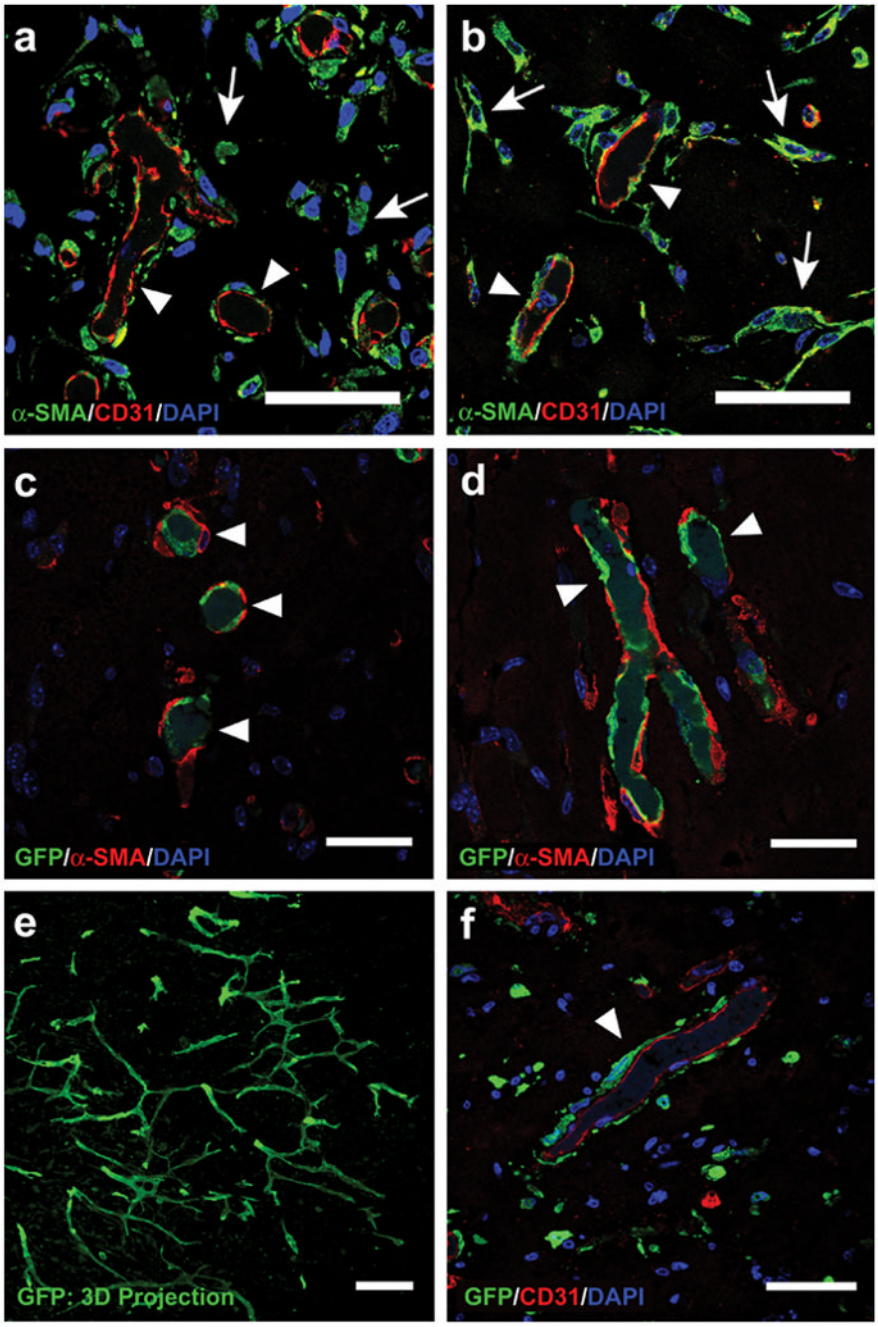

Figure 4. Specific location of EPCs and MPCs in the vascular bed

Matrigel implants containing cbEPCs and MPCs (40:60) were evaluated after one week. Implants with (a) bmMPCs and (b) cbMPCs produced lumenal structures that stained positive for human CD31, confirming that those lumens were formed by the implanted cells. In addition, α-SMA-expressing cells were detected both in the proximity (white arrows) and around the lumenal structures (white arrow heads), (scale bars, 50 μm). Implants that utilized GFP-labeled cbEPC and either (c) bmMPCs or (d) cbMPCs produced GFP-positive lumenal structures (white arrow heads) covered by α-SMA-expressing perivascular cells, confirming that cbEPCs were restricted to the luminal aspect of the vessels (scale bars, 30 μm). (e) Projections of whole-mount staining showed that the GFP-expressing cells formed

extensive networks throughout the implants (scale bar 100 μm). (f) Implants that utilized GFP-labeled bmMPC and unlabeled cbEPCs resulted in human CD31-positive lumenal structures with GFP-expressing cells adjacent to lumens (white arrow heads), confirming the role of MPCs as perivascular cells (scale bars, 50 μm). Images are representative of implants harvested from four different mice.

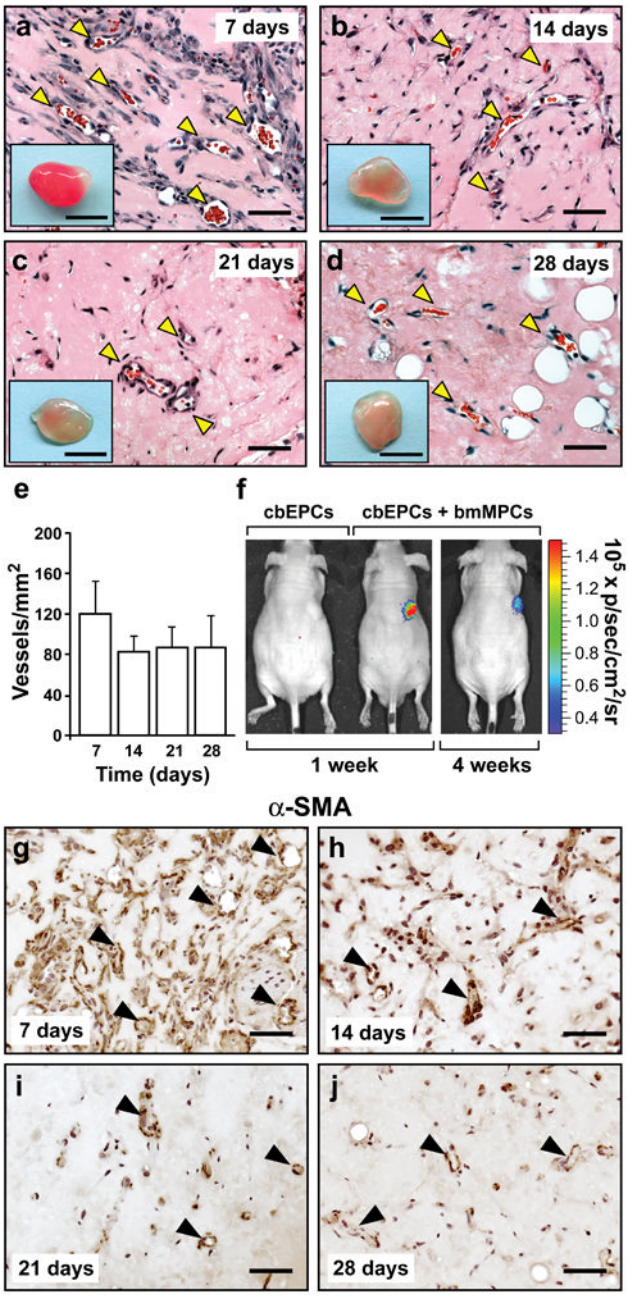

Figure 5. Durability of the vascular bed

Matrigel implants containing cbEPCs and bmMPCs (40:60) were injected subcutaneously on the back of six-week-old nu/nu mice. H&E staining showed lumenal structures containing erythrocytes (yellow arrow heads) in implants after (a) 7, (b) 14, (c) 21, and (d) 28 days (scale bars, 50 μm; macroscopic view of explanted Matrigel plugs shown in insets; insets scale bars, 5 mm). (e) Quantification of microvessel density was performed by counting erythrocyte-filled vessels. Each bar represents the mean microvessel density value determined from four separate implants and mice ± S.D. (vessels/mm^2). (f) Additional implants were prepared with luciferase-labeled cbEPC in the presence or absence of unlabeled bmMPCs. Mice were imaged using an IVIS Imaging System, and

bioluminescence detected 30-40 min after intraperitoneal injection of luciferin. In implants where cbEPCs and bmMPCs were co-implanted, bioluminescence was detected at 1 (image Min=-2.91×10^4., Max=2.67×10^5) and 4 (image Min=-3.29×10^4, Max=3.27×10^5) weeks, but not in those where cbEPCs were used alone. Immunohistochemical staining of α-SMA in implants after (g) 7, (h) 14, (i) 21, and (j) 28 days, revealed that α-SMA-expressing cells were progressively restricted to perivascular locations (black arrow heads), (scale bars, 50 μm). Images are representative of implants harvested from four different mice.

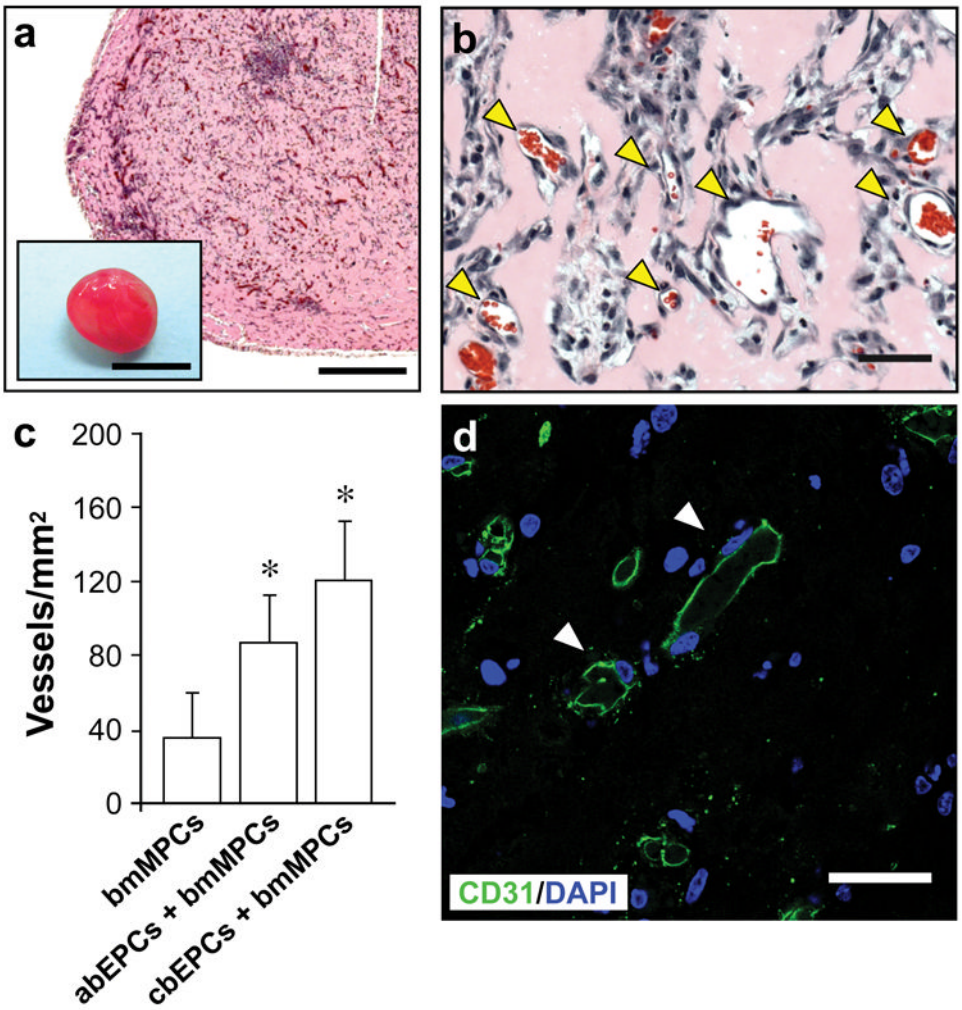

Figure 6. Vascular network formation using adult progenitor cells

Matrigel implants containing 40% abEPCs and 60% bmMPCs (obtained from human adult peripheral blood and adult bone marrow samples respectively) were injected subcutaneously on the back of six-week-old nu/nu mice and evaluated after one week. (a, b) H&E staining showed an uniform and extensive presence of lumenal structures containing erythrocytes (yellow arrow heads) throughout the implants (a scale bar, 500 μm; macroscopic view of explanted Matrigel plug shown in inset; inset scale bar, 5 mm; b scale bar, 50 μm). (c) Quantification of microvessel density was performed in implants seeded with bmMPCs in the absence or presence of either abEPCs or cbEPCs by counting erythrocyte-filled vessels. Each bar represents the mean microvessel density determined from four separate implants and mice ± S.D. (vessels/mm^2). * $P < .05$ compared to implants with bmMPCs alone (n=4). (d) Microvessels from implants containing 40% abEPCs and 60% bmMPCs stained positive for human CD31 (white arrow heads), confirming that those lumens were formed by the implanted cells (scale bars, 30 μm). Images are representative of implants harvested from four different mice.